Sensitivity of Tropical Extreme Precipitation to Surface Warming in Aquaplanet Experiments Using a Global Nonhydrostatic Model

Alejandro Uribe[1], Thorsten Mauritsen[2], and Jessica Vial[3]

[1]Stockholm University
[2]Department of Meteorology, Stockholm University
[3]LMD/IPSL, CNRS, Sorbonne University

November 24, 2022

Abstract

Increases of atmospheric water vapor holding capacity with temperature (7-8%Kˆ(-1), CC-rate) can lead to increasing Extreme Precipitation (EP). Observations show that tropical EP has increased during the last five decades with a rate higher than in the extratropics. Global climate models (GCM's) diverge in the magnitude of increase in the tropics, and cloud-resolving models (CRM's) indicate correlations between changes in tropical EP and organization of deep convection. We conducted global-scale aquaplanet experiments at a wide range of resolutions with explicit and parameterized convection to bridge the gap between GCM's and CRM's. We found increases of tropical EP beyond the CC rate, with similar magnitudes when using explicit convection and parametrized convection at the resolution it is tuned for. Those super-CC rates are produced due to strengthening updrafts where extreme precipitation occurs, and they do not exhibit relations with changes in convective organization.

Sensitivity of Tropical Extreme Precipitation to Surface Warming in Aquaplanet Experiments Using a Global Nonhydrostatic Model

Alejandro Uribe[1,2*], Jessica Vial[2,3], and Thorsten Mauritsen[1,2]

[1]University of Stockholm, Department of Meteorology, Stockholm, Sweden
[2]Max Planck Institute for Meteorology, Hamburg, Germany
[3]LMD/IPSL, CNRS, Sorbonne University, Paris, France

Key Points:

- The sensitivity of tropical extreme precipitation to warming is larger than the Clausius-Clapeyron rate
- Results are more sensitive to horizontal resolution when convection is parametrized than explicitly resolved
- Super Clausius-Clapeyron rates are mainly due to dynamical changes, but appear unrelated to changes in indicators of convective organization

*Current address: Department of Meteorology, Stockholm University, 106 91, Stockholm, Sweden.

Corresponding author: Alejandro Uribe, alejandro.uribe-cortes@misu.su.se

Abstract

Increases of atmospheric water vapor holding capacity with temperature ($7{-}8\%K^{-1}$, CC-rate) can lead to increasing Extreme Precipitation (EP). Observations show that tropical EP has increased during the last five decades with a rate higher than in the extratropics. Global climate models (GCM's) diverge in the magnitude of increase in the tropics, and cloud-resolving models (CRM's) indicate correlations between changes in tropical EP and organization of deep convection. We conducted global-scale aquaplanet experiments at a wide range of resolutions with explicit and parameterized convection to bridge the gap between GCM's and CRM's. We found increases of tropical EP beyond the CC rate, with similar magnitudes when using explicit convection and parametrized convection at the resolution it is tuned for. Those super-CC rates are produced due to strengthening updrafts where extreme precipitation occurs, and they do not exhibit relations with changes in convective organization.

Plain Language Summary

Theory and observations indicate tropical extreme precipitation might increase with global warming. Projections from climate models agree on increases in the extratropics, but not in the tropics. More idealized simulations indicate links between increases of tropical extreme precipitation and changes in the spatial organization of the meteorological systems producing those extremes. Using a novel model approach, we found that tropical extreme precipitation increases with warming more than expected due to increases in the dynamics of the extreme precipitation systems, whereas changes of the spatial organization have a small role.

1 Introduction

The Clausius-Clapeyron relation provides a theoretical starting point for understanding the response of extreme precipitation to a warming climate. At lower tropospheric temperatures this relation predicts a saturation specific humidity change of approximately $7 - 8\%K^{-1}$ (CC rate) (Trenberth et al., 2003). With such an increase of saturation water vapor in the atmosphere it is likely that the amount of precipitation from events where most of the water vapor precipitates out will increase with warming, and thus this value represents a basic scaling for the sensitivity of extreme precipitation to warming (Berg et al., 2013). This behavior of extreme precipitation events stands in contrast with global mean changes in precipitation with warming, which is instead linked to enhanced longwave cooling of the troposphere. This cooling is mostly balanced by enhanced convective heating through release of latent heat, leading to increasing mean global precipitation at a rate lower than, and not physically related to, the CC rate (Newell et al. (1975); Mitchell et al. (1987); Boer (1993)).

Observations provide evidence partly in favor of this scaling of extreme precipitation. Since the 1950s there have been statistically significant increases in the number of extreme precipitation events in more regions than there have been statistically significant decreases (Hartmann et al., 2013). However, observations indicate that sensitivities depend also on the type of precipitation with higher values than CC rate (super-CC) for convective precipitation (Berg et al., 2013). This discrepancy arises naturally between midlatitudes, where extreme precipitation is usually associated with frontal activity and midlatitude storms (Kodama et al., 2019), and the tropics where convection is the main driver. This was shown by O'Gorman (2015), who found that daily extremes in the tropics are more sensitive to climate warming than those in the extratropics and suggested one possible cause is from dynamical origin - changes in vertical motion.

General Circulation Model (GCM) simulations also produce a general increase of extremes, the strength of which depends on latitude (O'Gorman & Schneider, 2009b; O'Gorman, 2012). In models from the Coupled Model Intercomparison Project (CMIP) phase 3 for example, extratropical sensitivities consistently predict that precipitation extremes increase more slowly with surface air temperature than atmospheric water vapor content; however, tropical changes are not consistent among models, with sensitivities ranging from 1.3$\%K^{-1}$ to 30$\%K^{-1}$ (O'Gorman & Schneider, 2009a). These studies suggest that the discrepancy in the tropics may arise from inaccurate simulation of upward velocity during convection. Bhattacharya et al. (2017) suggested that to improve modeled tropical precipitation extremes, it is essential to better represent the upward velocity associated with those extremes. Increasing horizontal resolution may be a way to improve the simulation of convection in GCM's where precipitation is not resolved by the coarse grid and has to be parametrized. However, those convective parametrization schemes are sensitive to horizontal model resolution and time-step length (Li et al., 2011a, 2011b; Yang et al., 2014; Lu et al., 2014; Benedict et al., 2017; Williamson, 2013) and thus the sensitivity of extreme precipitation to warming varies not just among individual models but also across horizontal resolutions with a single model.

Given the long-standing structural uncertainties among CGM's, Cloud Resolving Models in idealized setups of Radiative-Convective Equilibrium (RCE) (Manabe and Strickler (1964); Nakajima and Matsuno (1988); Tompkins and Craig (1998)) have been used to study tropical convection and sensitivities of extreme precipitation to warming. On such setups and under certain conditions RCE can become unstable (Nilsson & Emanuel, 1999) and lead to spontaneous spatial organization of convection. In RCE simulations, it has been shown that extreme precipitation increases close to the CC rate if self-aggregation is absent (Romps, 2011; Muller et al., 2011) or if the degree of organization does not change (Bao et al., 2017); whereas super-CC behaviour has been found when self-aggregation increases with warming (Singleton & Toumi, 2013; Pendergrass et al., 2016; Bao et al., 2017; Bao & Sherwood, 2019).

Here we use a less idealized set of aquaplanet simulations to study the uncertainties of changes in tropical extreme precipitation by using a nonhydrostatic atmospheric GCM in rotating configuration with a meridional gradient of temperature (Neale & Hoskins, 2000; Medeiros et al., 2015). Model description and methods are presented in Section 2. In Section 3, we compare the sensitivity of tropical extreme precipitation to warming between simulations with parametrized and explicit convection and its resolution dependency, study contributors to those sensitivities, and look for relationships between the change of convective organization and the change of precipitation extremes. Finally, we present the conclusions in Section 4.

2 Model setup and methods

Simulations were performed using the ICOsahedral Nonhydrostatic Atmospheric general circulation model (ICON-A). ICON-A is built using the Max Planck Institute physical parametrization package, which originates from the ECHAM6.3 general circulation model (Mauritsen et al., 2019) and with adaptations to account for the change in the dynamical core and a new turbulence parametrization. A full description is given in Giorgetta et al. (2018).

The experiments were conducted using the aquaplanet configuration, which uses the Qobs zonally symmetric SST as surface boundary conditions (Neale & Hoskins, 2000). Owing to its simplicity (e.g. no topography, land-sea contrasts, surface heterogeneities), this configuration helps to understand the physical atmospheric processes driving the changes of extremes in response to global warming (Li et al., 2011a). Moreover, because diurnal insolation and the radiatively active species are held at equinoctial and hemispherically symmetric geometry, the model statistics are zonally and hemispherically symmetric, which helps to identify significant signals using relatively short integrations.

A range of simulations at different horizontal resolutions were performed with parametrization of convection on and off (explicit convection) for the control and uniformly increased SST of 4K (Table 1). We used explicit convection at resolutions lower than 10 km since even at coarse resolutions without parametrization of convection, models are able to pro-

Table 1. Experiment resolutions, time step lengths and cases with parameterized and explicit convection. The resolution is the approximate side length of squares with the same area as the average triangle in the ICON grid.

Grid name	Resolution [km]	Time step [min]	Parametrized	Explicit
R2B4	160	7.5	yes	yes
R2B5	80	3.75	yes	yes
R2B6	40	0.83	yes	yes
R2B8	10	0.25	no	yes

duce large scale features related to convection (Webb et al., 2015; Retsch et al., 2019). The simulations were initialized analytically and used time-invariant boundary conditions for SST, spectral solar irradiation, well mixed greenhouse gases CO2, CH4, N2O, CFC's and O3 concentration. All experiments were run for four years and we treated the first year as spin-up, except for $R2B8$ where the simulation length was limited to six months with one month of spin-up.

Daily zonal mean precipitation for explicit and parametrized experiments are shown in supporting information Figure S1. As is to be expected the global mean precipitation increases with warming, whereas the zonal distribution of precipitation follows a double ITCZ structure for explicit convection simulations. When resolution is increased, precipitation tends to be more zonally distributed with a displacement of the ITCZ away from the equator and an increase of midlatitude precipitation at the expense of tropical precipitation, particularly for R2B6 and R2B8. In general, however, the zonal distribution of precipitation in the parametrized convection experiments is somewhat erratic across resolutions, and the ITCZ behaviours in our experiments differ from those of Retsch et al. (2019) who used an earlier version of ICON-A and found a single ITCZ structure for explicit convection simulations at resolutions R2B4, R2B5 and R2B6, while a double ITCZ prevailed for parametrized convection. Since extremes in the tropics are more likely to occur within the ITCZ, simulated shifts in the large-scale tropical circulation might obscure our results and so in the following we shall discuss precipitation extremes in the entire tropics from $30°S$ and $30°N$.

To study changes in tropical Extreme Precipitation (EP) with warming, we define EP as the cases of grid points between $30°S$ to $30°N$ over the entire period exceeding the ith percentile of daily precipitation:

$$EP(i) = \frac{1}{n}\sum_{0}^{n} Pr_n \geq Pr_i, \tag{1}$$

where i varied from 99.9 to 99.99, Pr is daily precipitation and Pr_i is the ith percentile of daily precipitation. The selection of this metric allows us to capture the behaviour of the precipitation distribution tail instead of focusing on one particular percentile. With it we calculate the Sensitivity of tropical Extreme Precipitation to warming (SEP) as the fractional change in EP ($\delta EP(i)/EP(i)$) normalized by change in temperature (δT):

$$SEP(i) = \frac{\delta EP(i)}{\delta T \cdot EP(i)} = \frac{EP(i)_{4K} - EP(i)_{CTL}}{4K \cdot EP(i)_{CTL}}, \tag{2}$$

where the subscripts CTL and $4K$ denote control and 4K experiments, respectively.

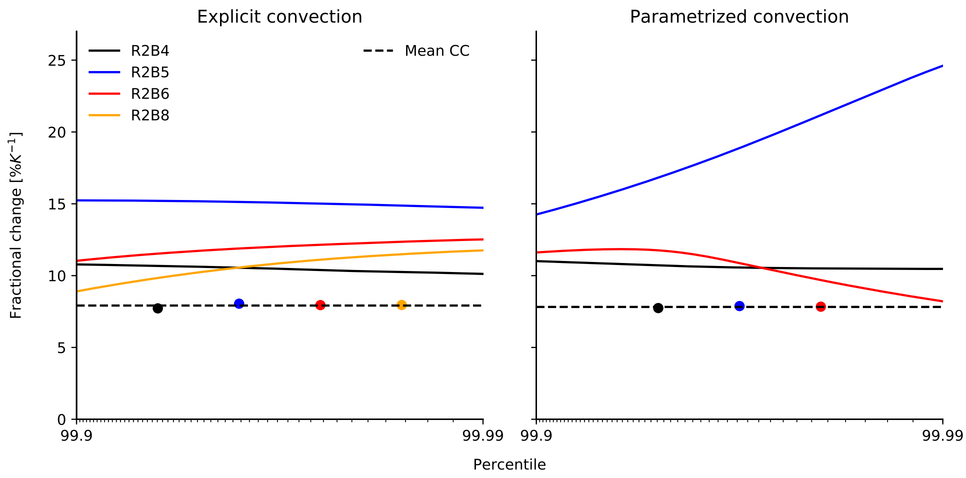

Figure 1. Solid lines show sensitivities of tropical extreme precipitation to warming. Fractional changes of lower tropospheric saturation specific humidity for each simulation are displayed as dots and the dashed line shows the mean across resolutions.

3 Results

3.1 Sensitivity of tropical extreme precipitation to warming

Sensitivities of tropical extreme precipitation to warming are displayed as solid lines in Figure 1. Extremes from both explicit and parametrized convection experiments increase with warming. For explicit convection simulations, sensitivities vary from $9\%K^{-1}$ to $15\%K^{-1}$ with a tendency to converge for the strongest extremes. This tendency is not clear for the experiments with parametrized convection, where at low resolution (R2B4) we observe a nearly constant sensitivity value, then at R2B5, it ranges from $14\%K^{-1}$ to $24\%K^{-1}$; and finally for the highest resolution (R2B6) it drops for the strongest extremes.

Fractional changes of lower tropospheric saturation specific humidity with warming in the tropics fall close to the CC rate (dots in Figure 1). In all simulations, extreme increases are higher than those fractional changes (super-CC, compare solid lines and dots). This suggests that not just increases in the capacity of the atmosphere to hold water vapor have an impact on extremes, but other processes contribute too. However, we note that for parametrized convection the amplitude of this difference varies with resolution more than it does for explicit convection. Since the convective parametrization implemented in ICON-A has been tuned for a grid resolution of R2B4, spurious behaviors at resolutions R2B5 and R2B6 resolutions might occur. This is mainly because the convective scheme is tuned to remove convective instability on a certain timescale. When resolution is increased from R2B4, the model dynamics may produce finer scale instabilities more rapidly than the parametrization can remove these, resulting in explicitly resolved updrafts or so-called grid-point storms (Williamson, 2013). We speculate that the erratic behavior of the higher resolution simulations is caused by the inadvertent competition between parameterized convection and partially resolved convective clouds. Given this, we restrain our analysis to explicit convection simulations and R2B4 with parametrized convection. Increases of extreme precipitation from parametrized convection at the resolution it is tuned for (R2B4) are similar to the increases with explicit convection, particularly to that at R2B4. This indicates a low model sensitivity of extreme precipitation changes with warming to the activation of convective parametrization for this resolution.

3.2 Contributors to increases of tropical extreme precipitation

Next we will use a scaling derived by Muller et al. (2011), which assumes that changes in precipitation efficiency with warming are negligible and separates changes in extremes in terms of changes in dynamics, through vertical motion (here pressure velocity, ω), and in thermodynamics, through the vertical gradient of saturation specific humidity, respectively. Derivation and testing of the scaling are presented in supporting information S1.

$$SEP \approx \underbrace{\frac{\left[\delta(\omega)\frac{\partial q_s}{\partial p}\right]}{\delta T \cdot \left[\omega \frac{\partial q_s}{\partial p}\right]}}_{Dynamic} + \underbrace{\frac{\left[\omega \delta \frac{\partial q_s}{\partial p}\right]}{\delta T \cdot \left[\omega \frac{\partial q_s}{\partial p}\right]}}_{Thermodynamic} . \qquad (3)$$

From the components of the scaling, we can identify that increases of tropical extreme precipitation derive from convective circulation strength through increases in ω and/or increases of vertical gradient of saturation specific humidity with warming, which are expected to follow the CC rate as long as the strongest vertical gradients of saturation specific humidity are located in the lower troposphere.

Results of the scaling (Equation 3) are displayed in Figure 2. We note a similar behaviour across resolutions with explicit convection and R2B4 with parametrized convection, in that increases of extreme precipitation result from both positive dynamics and thermodynamics contributions. In all simulations the dynamic contribution is positive, therefore contributing to the super-CC behavior of the model, whereas the thermodynamic contribution alone is close to the CC rate. It should be noted that the dynamic response exhibits a larger dependency on resolution when going from R2B4 to R2B5, than to the use of parametrization of convection, and that there is a nearly constant offset between the scaling and the actual sensitivities which might indicate either that the precipitation efficiency assumption is inaccurate or that other processes influence changes in tropical extreme precipitation.

3.3 Are sensitivities related to changes in convective organization?

We showed that tropical extreme precipitation increases with warming at rates higher than the CC rate and that strengthening of convective circulations when extremes occur leads to those super-CC tendencies in our experiments. As mentioned in Section 1, the amplitude of the sensitivity of tropical extreme precipitation to warming might be related to changes of convective organization whereby super-CC changes in extremes are correlated with increases of convective organization, and so we investigate if this is also the case in our simulations. To this end, we quantify the degree of convective organization in the tropics and its change with warming in a variety of ways: using subsiding fraction prime (SF´, Noda et al. (2019)) in the entire tropical band, as well as in smaller subdomains of varying sizes centered at the extreme event, and solely in the tropical band using organization index with eight point connectivity for resolutions R2B6 and R2B8 (Iorg, Tompkins and Semie (2017)) and an organization index with zero connectivity to include coarse resolutions ($\mathrm{Iorg}_{\text{-}0}$, Becker and Wing (2020)). A detailed description of the metrics is given in supporting information S2.

We found both increased and decreased tendencies of convective organization with warming (Figure 3). At high resolution (R2B5-8) all indices show a reduction in convective organization, whereas at coarse resolution (R2B4) convection tends to self-organise with warming in the areas where extremes occurs, while disorganise at large scale (we obtained similar results for coarse grained resolutions to R2B4, see Figure S6). Those

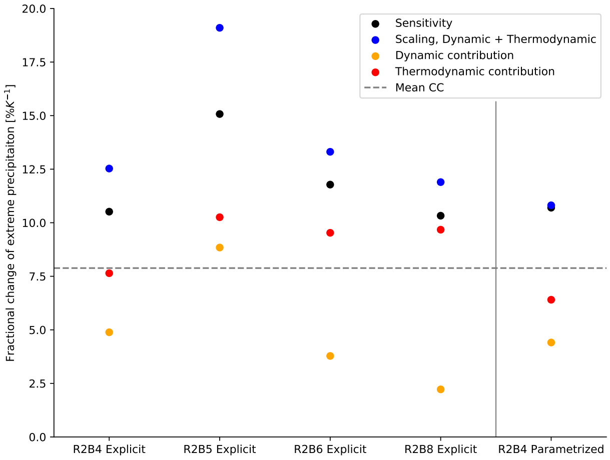

Figure 2. Sensitivity of tropical extreme precipitation to warming (black), scaling (blue) and contributions to sensitivities from dynamics (yellow) and thermodynamic (red). Values are calculated by averaging the extremes interval (99.9 to 99.99). The dashed grey line indicates the mean fractional change of lower tropospheric saturation specific humidity across simulations and the vertical line separates explicit convection experiments from parametrized convection at R2B4.

results are in agreement with Muller and Held (2012) who found that self-organization of convection is favored by coarse resolution but opposite to Bao et al. (2017), Singleton and Toumi (2013) and Pendergrass et al. (2016) where increases of extremes correlate with self-organization. This discrepancy across resolutions suggests that changes in tropical convective organization have a negligible impact on changes of tropical extreme precipitation with warming in our simulations.

4 Conclusions

Aquaplanet simulations with the ICON-A model are performed to explore the sensitivity of tropical extreme precipitation to warming across a wide range spatial resolutions with and without parametrization of convection. We find positive sensitivities with amplitudes larger than the increase of lower tropospheric saturation specific humidity, or CC rate, at all resolutions. Results from explicit convection simulations converge for the strongest precipitation extremes, whereas for parameterized convection simulations, the sensitivities strongly vary with horizontal resolution, although results from R2B4 are similar to those from the explicit convection simulations. We suggest this occurs since the parametrization scheme used in ICON-A was tuned for that particular resolution.

We next investigate whether dynamical changes can explain the super-CC behaviour of tropical extreme precipitation using a diagnostic framework. In all simulations we find positive contributions from dynamics, resulting in stronger updrafts where extreme precipitation occurs. Nevertheless, thermodynamical changes resulting from changes in the vertical gradient of saturation specific humidity also contributes relative to the simple CC-scaling in the higher resolution explicit simulations, but not in the coarse resolution simulations (R2B4). Furthermore, it should be noted that there is a considerable residual in the diagnosed changes, suggesting that assuming invariant precipitation efficiency is inaccurate or that other processes might be involved.

Finally, we explore whether convective organization could be involved using an array of indices that in various ways characterise the degree of organization. We find somewhat surprisingly in most cases organisation decreases with warming: in the explicit con-

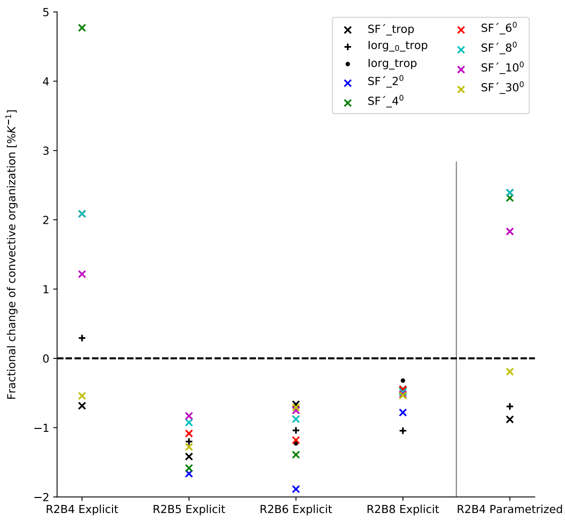

Figure 3. Fractional changes of organization metrics for large scale (SF´_trop, Iorg$_0$_trop and Iorg_trop) and for subdomains centered where extremes occur (SF´$_{30}$, SF´$_{10}$, SF´$_8$, SF´$_6$, SF´$_4$ and SF´$_2$). The vertical line separates explicit convection experiments from parametrized convection at R2B4. Note that, given the resolution of R2B4, a subdomain of 2° x 2° will contain a unique grid point and the fractional change of SF´ will be zero; and subdomains from 6° x 6° and 8° x 8° will contain the same amount of grid points, producing equal fractional changes.

vection simulations with 10-80 km resolution (R2B5-8) it decreases by about 1$\%K^{-1}$. In the two simulations with 160 km (R2B4) convection disorganizes at large scale; but self-organizes in the areas where extremes occur. It is concluded that convective organization played either no or a negligible role in causing the model's super-CC behaviour of tropical extreme precipitation.

Acknowledgments

The authors are grateful to Caroline Muller, Addisu Semie, Allison Wing and Frida Bender who provided useful comments and suggestions. We would like to thank Clare Flynn for her helpful English revision. The study was supported by the Max Planck Society for the advancement of science, the European Research Council (highECS (grant no. 770765) and CONSTRAIN (grant no. 820829)). Computational resources were made available by Deutsches Klimarechenzentrum (DKRZ) through support from Bundesministerium für Bildung und Forschung (BMBF) and by the Swedish National Infrastructure for Computing (SNIC) at the PDC Center for High Performance Computing, KTH Royal Institute of Technology. The primary data for this study, that is, the ICON-A model is described in Giorgetta et al. (2018) and its source code and components are available on https://mpimet.mpg.de/en/science/modeling-with-icon/code-availability. The configuration scripts to run the model, the data and scripts to reproduce the figures can be found in Uribe et al. (2020).

References

Bao, J., & Sherwood, S. C. (2019). The Role of Convective Self-Aggregation in Extreme Instantaneous Versus Daily Precipitation. *Journal of Advances in Modeling Earth Systems*, *11*(1), 19-33. doi: 10.1029/2018MS001503

Bao, J., Sherwood, S. C., Colin, M., & Dixit, V. (2017). The Robust Relationship Between Extreme Precipitation and Convective Organization in Idealized Numerical Modeling Simulations. *Journal of Advances in Modeling Earth Systems*, *9*(6), 2291-2303. doi: 10.1002/2017MS001125

Becker, T., & Wing, A. A. (2020). Understanding the Extreme Spread in Climate Sensitivity within the Radiative-Convective Equilibrium Model Intercomparison Project. *Journal of Advances in Modeling Earth Systems*, *12*(10), e2020MS002165. doi: 10.1029/2020MS002165

Benedict, J. J., Medeiros, B., Clement, A. C., & Pendergrass, A. G. (2017). Sensitivities of the hydrologic cycle to model physics, grid resolution, and ocean type in the aquaplanet Community Atmosphere Model. *Journal of Advances in Modeling Earth Systems*, *9*(2), 1307-1324. doi: 10.1002/2016MS000891

Berg, P., Moseley, C., & Haerter, J. O. (2013). Strong increase in convective precipitation in response to higher temperatures. *Nature Geoscience*. doi: 10.1038/ngeo1731

Bhattacharya, R., Bordoni, S., & Teixeira, J. (2017). Tropical precipitation extremes: Response to SST-induced warming in aquaplanet simulations. *Geophysical Research Letters*, *44*(7), 3374-3383. doi: 10.1002/2017GL073121

Boer, G. J. (1993). Climate change and the regulation of the surface moisture and energy budgets. *Climate Dynamics*, *8*(5), 225–239. doi: 10.1007/BF00198617

Giorgetta, M. A., Brokopf, R., Crueger, T., Esch, M., Fiedler, S., Helmert, J., ... Stevens, B. (2018). ICON-A, the Atmosphere Component of the ICON Earth System Model: I. Model Description. *Journal of Advances in Modeling Earth Systems*, *10*(7), 1613-1637. doi: 10.1029/2017MS001242

Hartmann, D., Tank, A. K., Rusticucci, M., Alexander, L., Brönnimann, S., Charabi, Y., ... Zhai, P. (2013). *Observations: Atmosphere and Surface. In: Climate Change 2013: The Physical Science Basis. Contribution of Working Group I to the Fifth Assessment Report of the Intergovernmental Panel on Climate Change.* Cambridge, United Kingdom and New York, NY, USA: Cambridge University Press.

Kodama, C., Stevens, B., Mauritsen, T., Seiki, T., & Satoh, M. (2019). A New Perspective for Future Precipitation Change from Intense Extratropical Cyclones. *Geophysical Research Letters*, *46*(21), 12435-12444. doi: 10.1029/2019GL084001

Li, F., Collins, W. D., Wehner, M. F., Williamson, D. L., & Olson, J. G. (2011b). Response of precipitation extremes to idealized global warming in an aqua-planet climate model: towards a robust projection across different horizontal resolutions. *Tellus A*, *63*(5), 876-883. doi: 10.1111/j.1600-0870.2011.00543.x

Li, F., Collins, W. D., Wehner, M. F., Williamson, D. L., Olson, J. G., & Algieri, C. (2011a). Impact of horizontal resolution on simulation of precipitation extremes in an aqua-planet version of Community Atmospheric Model (CAM3). *Tellus A: Dynamic Meteorology and Oceanography*, *63*(5), 884-892. doi: 10.1111/j.1600-0870.2011.00544.x

Lu, J., Ruby Leung, L., Yang, Q., Chen, G., Collins, W. D., Li, F., ... Feng, X. (2014). The robust dynamical contribution to precipitation extremes in idealized warming simulations across model resolutions. *Geophysical Research Letters*, *41*(8), 2971-2978. doi: 10.1002/2014GL059532

Manabe, S., & Strickler, R. F. (1964). Thermal Equilibrium of the Atmosphere with a Convective Adjustment. *Journal of the Atmospheric Sciences*, *21*(4), 361-385. doi: 10.1175/1520-0469(1964)021⟨0361:TEOTAW⟩2.0.CO;2

Mauritsen, T., Bader, J., Becker, T., Behrens, J., Bittner, M., Brokopf, R., ... Roeckner, E. (2019). Developments in the MPI-M Earth System Model version 1.2 (MPI-ESM1.2) and Its Response to Increasing CO2. *Journal of Advances in Modeling Earth Systems*, *11*(4), 998-1038. doi: 10.1029/2018MS001400

Medeiros, B., Stevens, B., & Bony, S. (2015). Using aquaplanets to understand the robust responses of comprehensive climate models to forcing. *Climate Dynamics*, *44*. doi: 10.1007/s00382-014-2138-0

Mitchell, J. F. B., Wilson, C. A., & Cunnington, W. M. (1987). On Co2 climate sensitivity and model dependence of results. *Quarterly Journal of the Royal Meteorological Society*, *113*(475), 293-322. doi: 10.1002/qj.49711347517

Muller, C. J., & Held, I. M. (2012, 08). Detailed Investigation of the Self-Aggregation of Convection in Cloud-Resolving Simulations. *Journal of the Atmospheric Sciences*, *69*(8), 2551-2565. doi: 10.1175/JAS-D-11-0257.1

Muller, C. J., O'Gorman, P. A., & Back, L. E. (2011). Intensification of Precipitation Extremes with Warming in a Cloud-Resolving Model. *Journal of Climate*, *24*(11), 2784-2800. doi: 10.1175/2011JCLI3876.1

Nakajima, K., & Matsuno, T. (1988). Numerical Experiments Concerning the Origin of Cloud Clusters in the Tropical Atmosphere. *Journal of the Meteorological Society of Japan. Ser. II*, *66*(2), 309-329. doi: 10.2151/jmsj1965.66.2_309

Neale, R. B., & Hoskins, B. J. (2000). A standard test for AGCMs including their physical parametrizations: I: the proposal. *Atmospheric Science Letters*, *1*(2), 101-107. doi: 10.1006/asle.2000.0022

Newell, R. E., Hernan, G. F., Gould-Stewart, S., & Tanaka, M. (1975). Decreased global rainfall during the past Ice Age. *Nature*, *253*(5486), 33–34. doi: 10.1038/253033b0

Nilsson, J., & Emanuel, K. A. (1999). Equilibrium atmospheres of a two-column radiative-convective model. *Quarterly Journal of the Royal Meteorological Society*, *125*(558), 2239-2264. doi: 10.1002/qj.49712555814

Noda, A. T., Kodama, C., Yamada, Y., Satoh, M., Ogura, T., & Ohno, T. (2019). Responses of Clouds and Large-Scale Circulation to Global Warming Evaluated From Multidecadal Simulations Using a Global Nonhydrostatic Model. *Journal of Advances in Modeling Earth Systems*, *11*(9), 2980-2995. doi: 10.1029/2019MS001658

O'Gorman, P. A. (2012). Sensitivity of tropical precipitation extremes to climate change. *Nature Geoscience*, *5*. doi: 10.1038/ngeo1568

O'Gorman, P. A. (2015). Precipitation Extremes Under Climate Change. *Current Climate Change Reports*. doi: 10.1007/s40641-015-0009-3

O'Gorman, P. A., & Schneider, T. (2009a). The physical basis for increases in precipitation extremes in simulations of 21st-century climate change. *Proceedings of the National Academy of Sciences*. doi: 10.1073/pnas.0907610106

O'Gorman, P. A., & Schneider, T. (2009b). Scaling of Precipitation Extremes over a Wide Range of Climates Simulated with an Idealized GCM. *Journal of Climate*, *22*(21), 5676-5685. doi: 10.1175/2009JCLI2701.1

Pendergrass, A. G., Reed, K. A., & Medeiros, B. (2016). The link between extreme precipitation and convective organization in a warming climate: Global radiative-convective equilibrium simulations. *Geophysical Research Letters*, *43*(21), 11,445-11,452. doi: 10.1002/2016GL071285

Retsch, M. H., Mauritsen, T., & Hohenegger, C. (2019). Climate Change Feedbacks in Aquaplanet Experiments With Explicit and Parametrized Convection for Horizontal Resolutions of 2,525 Up to 5 km. *Journal of Advances in Modeling Earth Systems*, *11*(7), 2070-2088. doi: 10.1029/2019MS001677

Romps, D. M. (2011). Response of Tropical Precipitation to Global Warming. *Journal of the Atmospheric Sciences*, *68*(1), 123-138. doi: 10.1175/2010JAS3542.1

Singleton, A., & Toumi, R. (2013). Super-Clausius–Clapeyron scaling of rainfall in a model squall line. *Quarterly Journal of the Royal Meteorological Society*, *139*(671), 334-339. doi: 10.1002/qj.1919

Tompkins, A. M., & Craig, G. C. (1998). Radiative–convective equilibrium in a three-dimensional cloud-ensemble model. *Quarterly Journal of the Royal Meteorological Society*, *124*(550), 2073-2097. doi: 10.1002/qj.49712455013

Tompkins, A. M., & Semie, A. G. (2017). Organization of tropical convection in low vertical wind shears: Role of updraft entrainment. *Journal of Advances in Modeling Earth Systems*, *9*(2), 1046-1068. doi: 10.1002/2016MS000802

Trenberth, K. E., Dai, A., Rasmussen, R. M., & Parsons, D. B. (2003). The Changing Character of Precipitation. *Bulletin of the American Meteorological Society*, *84*(9), 1205-1218. doi: 10.1175/BAMS-84-9-1205

Uribe, A., Vial, J., & Mauritsen, T. (2020, December). *Replication Data for experiments and figures in: Sensitivity of Tropical Extreme Precipitation to Surface Warming in Aquaplanet Experiments Using a Global Nonhydrostatic Model.* Zenodo. Retrieved from `https://doi.org/10.5281/zenodo.4114123` doi: 10.5281/zenodo.4114123

Webb, M. J., Lock, A. P., Bretherton, C. S., Bony, S., Cole, J. N. S., Idelkadi, A., ... Zhao, M. (2015). The impact of parametrized convection on cloud feedback. *Philosophical transactions. Series A, Mathematical, physical, and engineering sciences*, *373*. doi: 10.1098/rsta.2014.0414

Williamson, D. L. (2013). The effect of time steps and time-scales on parametrization suites. *Quarterly Journal of the Royal Meteorological Society*, *139*(671), 548-560. doi: 10.1002/qj.1992

Yang, Q., Leung, L. R., Rauscher, S. A., Ringler, T. D., & Taylor, M. A. (2014). Atmospheric Moisture Budget and Spatial Resolution Dependence of Precipitation Extremes in Aquaplanet Simulations. *Journal of Climate*, *27*(10), 3565-3581. doi: 10.1175/JCLI-D-13-00468.1

Supporting Information for "Sensitivity of Tropical Extreme Precipitation to Surface Warming in Aquaplanet Experiments Using a Global Nonhydrostatic Model"

Contents of this file

S1. Derivation of the scaling of sensitivity of tropical extreme precipitation to warming

We start from the definition of liquid ice water static energy (h_L) and total ice water

---

mixing ratio q_T:

$$h_L = h - L_v q_T, \quad (1)$$

$$q_T = q + q_r + q_c + q_s + q_g + q_i + l, \quad (2)$$

where h is moist static energy, L_v is latent heat of vaporization, q is water vapor mixing ratio, q_r is rain mixing ratio, q_c is cloud water mixing ratio, q_s is snow mixing ratio, q_g graupel mixing ratio, q_i is cloud ice mixing ratio and l is liquid water mixing ratio. We have neglected the differences between latent heat of vaporization and sublimation ($L_v \approx L_S$).

Having $h = s + L_v q$, where s is dry static energy, and replacing equation 2 in equation 1 we have:

$$h_L = s - L_v(q_r + q_c + q_s + q_g + q_i) - L_v l. \quad (3)$$

Since h_L is conserved in adiabatic fluid parcel displacements:

$$\left[\frac{Dh_L}{Dt}\right] = \left[\frac{Ds}{Dt}\right] - L_v \left[\frac{D(q_r + q_c + q_s + q_g + q_i)}{Dt}\right] - L_v P = 0, \quad (4)$$

where $P = Dl/Dt$ is surface precipitation and the square brackets denote vertical integration:

$$[\cdots] = -\int_{surface}^{100hPa} (\cdots)\frac{dp}{g}. \quad (5)$$

Thus:

$$\left[\frac{Ds}{Dt}\right] = L_v \left[\frac{D(q_r + q_c + q_s + q_g + q_i)}{Dt}\right] + L_v P. \quad (6)$$

The left side of equation 6 can be written as:

$$\left[\frac{Ds}{Dt}\right] = \left[\frac{\partial s}{\partial t}\right] + \left[u\frac{\partial s}{\partial x}\right] + \left[v\frac{\partial s}{\partial y}\right] + \left[-\omega\frac{\partial s}{\partial p}\right], \quad (7)$$

where u, v and ω are zonal wind, meridional wind and pressure velocity, respectively. When extreme precipitation occurs, vertical advection (last term on the right side of equation 7) is the main contributor to the budget for all resolutions with explicit convection and for R2B4 and R2B5 with parametrized convection (Figure S2). In those resolutions, we can approximate the tendency equation of dry static energy by the vertical advection term:

$$\left[\frac{Ds}{Dt}\right] \approx -\left[\omega\frac{\partial s}{\partial p}\right]. \tag{8}$$

On the other hand, when extremes occur, specific humidity approximates the saturation specific humidity for all explicit convection simulations and for R2B4 with parametrized convection. (For the rest of the resolutions with parametrized convection, the atmospheric lapse rate is not restored to its equilibrium state). At those resolutions where this assumption is met, and given the conservation of moist static energy we can write:

$$ds \approx -L_v dq_s. \tag{9}$$

Using this assumption we tracked if the vertically integrated advection of dry static energy is approximated by minus latent heat times the vertical integrated advection saturation specific humidity (equation 10). Figure S4 shows the confirmation of this assumption.

$$\left[\omega\frac{ds}{dp}\right] \approx -L_v\left[\omega\frac{dq_s}{dp}\right]. \tag{10}$$

Introducing equation 10 in equation 8 and using equation 6 to solve for $EP(i)$ (we substitute P by $EP(i)$ since the assumptions are met just for extreme precipitation values), we have:

$$EP(i) \approx \left[w\frac{\partial q_s}{\partial p}\right] - \left[\frac{D(q_r + q_c + q_s + q_g + q_i)}{Dt}\right] \tag{11}$$

Now, we define a precipitation efficiency:

$$\epsilon = 1 - \frac{\left[\frac{D(q_r+q_c+q_s+q_g+q_i)}{Dt}\right]}{\left[w\frac{\partial q_s}{\partial p}\right]}. \quad (12)$$

Finally we get the scaling as the product of precipitation efficiency ϵ and total condensation:

$$EP(i) \approx \epsilon \left[w\frac{\partial q_s}{\partial p}\right]. \quad (13)$$

We test the scaling (equation 13) by computing correlations between the total condensation term and the actual extreme precipitation in our CTL and 4K simulations (Figure S5). As expected from the above assumptions we found that the scaling reproduces the behaviour of extreme precipitation for all resolutions with explicit convection and for R2B4 with parametrized convection.

Using this EP scaling and neglecting changes in precipitation efficiency a SEP can be derived in terms of changes in dynamics and thermodynamics through omega and vertical gradient of saturation specific humidity, respectively.

$$SEP(i) = \frac{\delta EP(i)}{\delta T \cdot EP(i)} \approx \underbrace{\frac{\left[\delta(\omega)\frac{\partial q_s}{\partial p}\right]}{\delta T \cdot \left[\omega\frac{\partial q_s}{\partial p}\right]}}_{Dynamic} + \underbrace{\frac{\left[\omega\delta\frac{\partial q_s}{\partial p}\right]}{\delta T \cdot \left[\omega\frac{\partial q_s}{\partial p}\right]}}_{Thermodynamic}. \quad (14)$$

S2. Convective organization metrics.

1. Subsiding fraction prime (SF´): The development of convective aggregation in GCM is closely associated with the tendency of the atmosphere to develop large areas of dry, subsiding air, and the tendency of convection to clump within narrow areas of large-scale ascents. SF´ is designed to measure the degree of convective organization in simulations with background circulation (i.e Hadley circulation) that has to be excluded to more

appropriately measure the behavior of individual cumulus convection. To remove the background circulation, the tropics is divided into squared subdomains of 10° longitude and the mean of omega over each subdomain is computed. Then, SF´ is defined as the fractional coverage of negative ω', where $\omega' = \omega - < \omega >$ at each subdomain.

2. Organization index (Iorg): A simple organization index that permits to classify a field as regular, random or clustered. We use a threshold of omega higher or equal to the mean subsiding omega at the level of 500 hPa to distinguish convective grid cells. Then, to identify convective grid cells that are part of the same cluster, eight point connectivity is employed in resolutions R2B6 and R2B8.

3. Organization index with zero connectivity ($Iorg_{-0}$): For low resolutions the minimum distance to cluster by vicinity used by Iorg is too large and the resulting clusters might not represent individual convective systems. To avoid this issue we identify convective grids cell as individual entities using zero connectivity.

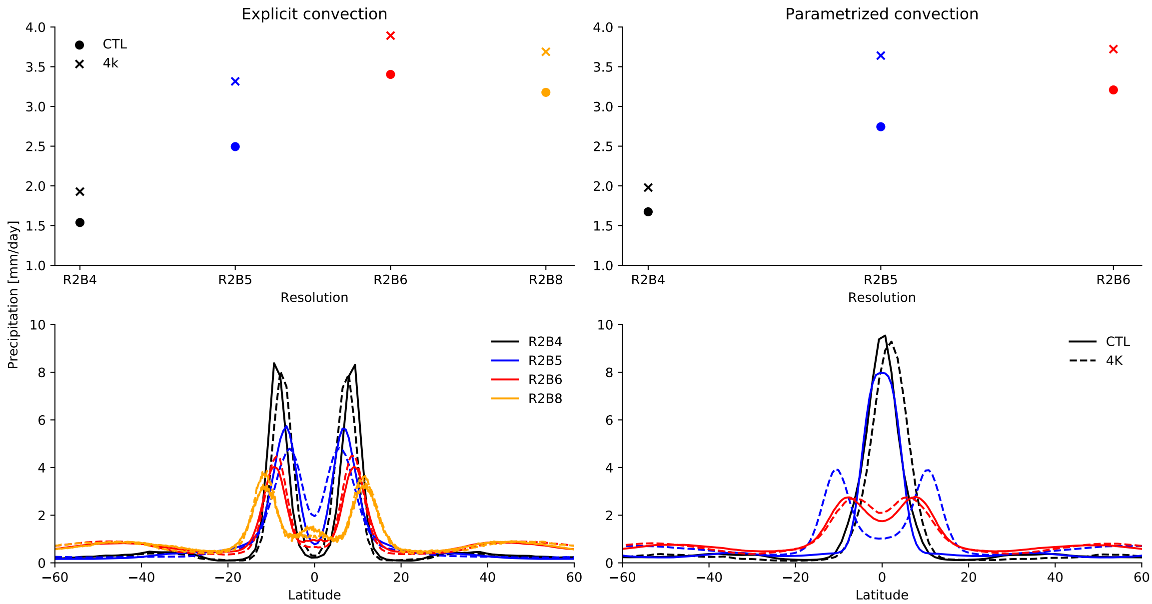

Figure S1. Global mean precipitation (top) and zonal mean precipitation normalized by global mean (bottom). For the comparison, we used a mass-conserving interpolation method to aggregate the results to the coarsest resolution (R2B4) in order to distinguish between the effect of grid size and change in physical processes

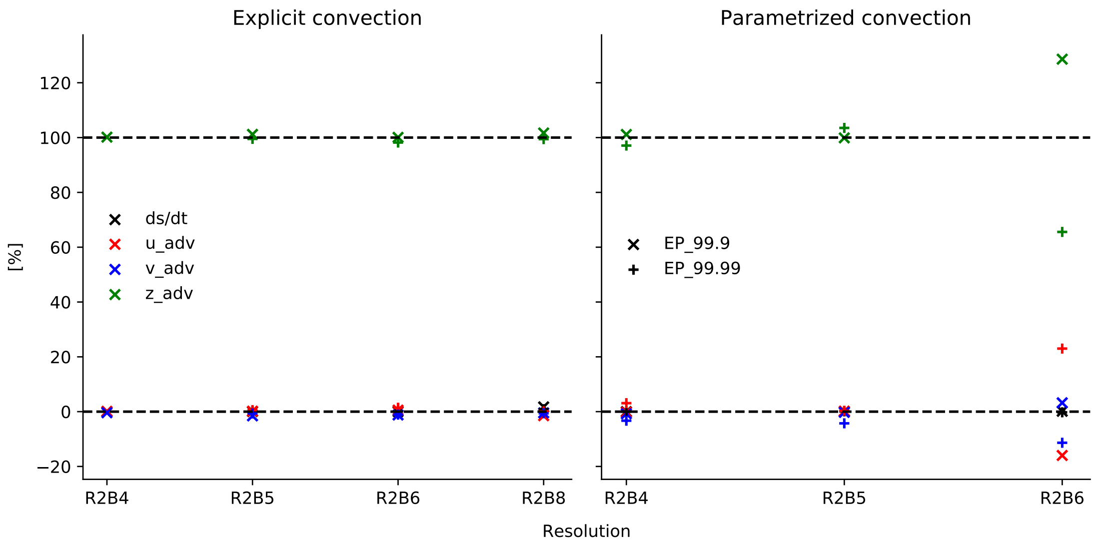

Figure S2. Relative proportion of local change (black), zonal advection (red) meridional advection (blue) and vertical advection (green) of vertical integrated dry static energy to the total vertical integrated material derivative of dry static energy when $EP_{99.9}$ ("x") and $EP_{99.99}$ ("+") occurs.

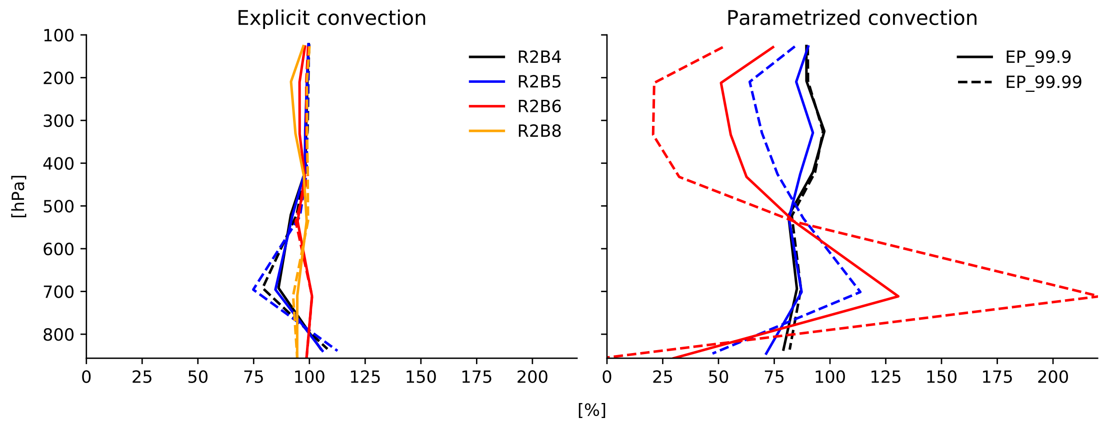

Figure S3. Ratio of specific humidity to saturation specific humidity profiles when $EP_{99.9}$ (solid) and $EP_{99.99}$ (dashed) occurs.

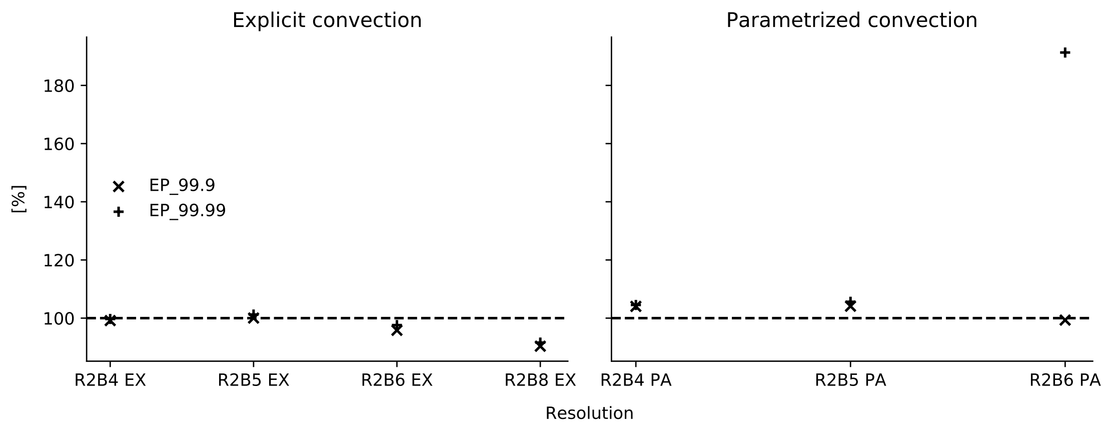

Figure S4. Ratio of negative latent heat times vertical integrated advection of saturation specific humidity to vertical integrated advection of dry static energy when $EP_{99.9}$ ("x") and $EP_{99.99}$ ("+") occurs.

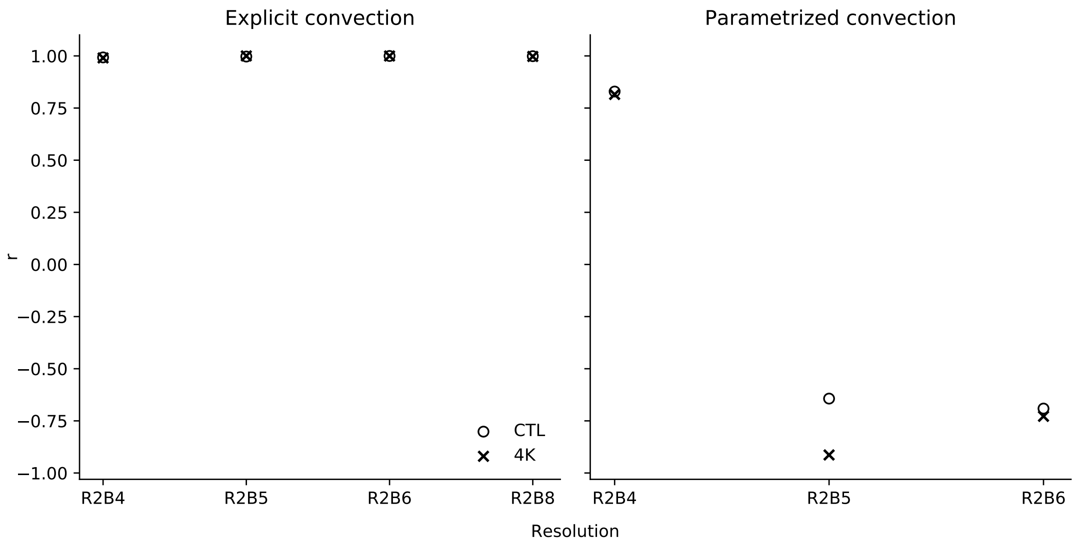

Figure S5. Correlation between total condensation and extreme precipitation.

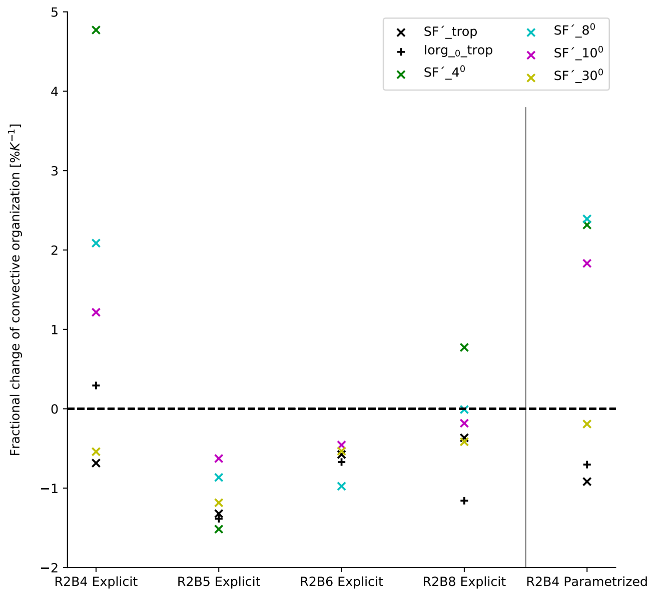

Figure S6. Fractional changes of organization metrics for large scale (SF´_trop and Iorg$_{-0-}$trop) and for subdomains centered where extremes occurs (SF´$_{-30}$, SF´$_{-10}$, SF´$_{-8}$, and SF´$_{-4}$) at coarse grained resolutions to R2B4. Note that, given the resolution of R2B4, a subdomain of 2° x 2° will contain a unique grid point and the fractional change of SF´ will be zero; and subdomains from 6° x 6° and 8° x 8° will contain the same amount of grid points, producing equal fractional changes.